Received: 25 May 2020 | Accepted: 17 August 2020

DOI: 10.1002/asna.202013815

Astronomische Nachrichten

ORIGINAL ARTICLE

Astrometric observations of visual binaries using 26-inch refractor at Pulkovo Observatory during 2014–2019

Igor Izmailov[1] | **Aleksey Rublevsky**[2] | **Arina Apetyan**[1]

[1]Central Astronomical Observatory at Pulkovo, Russian Academy of Sciences, Saint Petersburg, Russia

[2]Crimean Astrophysical Observatory, Russian Academy of Sciences, Crimea, Nauchny, Russia

Correspondence
Arina Apetyan, Pulkovskoye Shosse, 65, Saint Petersburg, 196140, Russia.
Email: aaapetyan@gmail.com

Funding information
Russian Foundation for Basic Research, Grant/Award Number: 20-02-00563A

Abstract

We present 18,365 astrometric observations of 290 visual binaries obtained with the 26-inch refractor of Pulkovo Observatory during 2014–2019. The separation between components is from 1″.3 to 37″ with a median value of 4″.8. For a single observation, the mean separation error is 0″.013, and the mean position angle error is 0°.44/ρ, where ρ is an angular distance in arcseconds. We compare the observations of sample stars with the data from the Gaia DR2 catalog and the results of the ground-based observations performed with other telescopes.

KEYWORDS

binaries: visual, methods: observational

1 | INTRODUCTION

This paper continues a series of studies presenting results of visual binaries' observations made with the 26-inch Pulkovo refractor. The first light image for the refractor was obtained using a photographic plate on April 19, 1956. For the last six decades, the observations were performed with this telescope on almost every clear night except for short breaks caused by technical difficulties. A large part of the observation time has always been allotted to the visual binaries observation program. Initially, the observations were carried out using photographic plates. In 1996, the refractor was equipped with the charge-coupled device (CCD)-camera ST-6, which had a main disadvantage of a narrow field of view—approximately $3' \times 2'$—whereas the size of a pixel in angular terms was $0''.53 \times 0''.46$. Even though CCD-observations delivered better accuracy, photographic observations had been performed up until 2007 when the last astronegative was obtained. First, using these two approaches simultaneously allowed us to derive systematic differences in relative positions, which in some cases exceed random errors significantly. Second, this framework enabled the determination of the orbits of visual binaries using the apparent motion parameters (AMP) method back in 2009–2012 (Kiselev & Romanenko 2011; Kiselev et al. 2009, 2012; Kisselev et al. 2009; Romanenko & Kiselev 2014; Shakht et al. 2010). If only the results of CCD-observations were used, the orbit determination would have been postponed. When photographic observations stopped in 2007, the refractor was also equipped with the FLI ProLine 09000 CCD-camera (more information about it will be presented later in the paper).

The program of observing binaries at the 26-inch refractor is focused on defining orbits using the AMP method that requires a dense homogeneous series of observations. Therefore, this program includes a small sample of several hundred pairs. To improve accuracy, we observe each of those pairs from 5 to 20 times per year depending on the changes in relative positions in the pair. There is another approach when orbits are defined mainly based on the apparent ellipse. In this case, it is more effective to survey a large number of binaries and detect mostly close pairs

that show a bigger relative motion (see Mason et al. (2018), Tokovinin et al. (2019)).

In Izmailov (2019), the Thiele-Innes method was implied. Its disadvantage, compared to the AMP method, is using only positions without taking radial velocities into account. Besides, for some wide binaries, relative radial accelerations recently became available in the context of a search for exoplanets using the radial velocities approach (see Trifonov et al. 2020). Thus, there is an opportunity to create a new orbit determination methodology that would combine the advantages of both the Thiele-Innes and the AMP methods. Because the Gaia project (Brown et al. (2018)) achieves better accuracy of wide binaries' relative positions than ground-based observations, the observation program formation will be fundamentally revised when this new method is developed. In particular, we plan to adopt techniques based on speckle interferometry for close binaries observations, which would be resolved in the Gaia catalog.

2 | OBSERVATIONS AND PROCESSING

In this paper, we present the results of the observations obtained from April 12, 2014 to December 11, 2019. For 739 nights, 18,365 single observations were performed, including pointing and imaging. Utilization of clear nights is 80%, which is a good result. The remaining 20% were lost mainly due to a problematic technical state of the telescope. The 26-inch Pulkovo refractor with a focal length of 10,400 mm provides a scale of 0.238″ per pixel. The observations were made using CCD-cameras FLI ProLine 09000 with 12-mkm pixels, which sets up a $12' \times 12'$ field of view. The observations were fully automated. In case of malfunctions, dome flaps would close automatically, and a signal of the need for observer intervention would be sent. Automation principles for this telescope are described in Izmailov et al. (2004).

The observation process was organized in a way where 10 min were allocated to each star: 5 min for pointing and centering and 5 min for imaging. The apparent magnitudes of the observed stars range from 3.5^m to 13^m; therefore, exposure times were from 0.01 to 45 s. The separations between components are from 1″.3 to 37″, with a median value of 4″.8.

The preliminary processing of CCD images included accounting for dark current and flat field variations. Star images centers were calculated using the IZMCCD package.[1] The Moffat profile (Moffat (1969)) was used to approximate the images:

$$I(x,y) = D + \frac{C}{(1+Ar^2)^{\alpha}},$$

$$r^2 = (x-x_0)^2 + (1+B)(y-y_0)^2 + E(x-x_0)(y-y_0),$$

where the variables are as follows: x, y are the integer values of representing the pixel location in each direction, I is the pixel reading at (x,y), x_0, y_0, A, B, C, D, E are the defined model parameters, r is the scaled distance between (x, y) and (x_0, y_0).

In this approach, each pixel with coordinates (x, y) corresponds to one equation. A pixel is considered a part of the star image if it is located within a certain radius of the preliminary center, that is, circular apertures were implemented. For each star, the radius is selected individually in the range from 5 to 10 pixels depending on the exposure and brightness. To minimize systematic errors, the same radius value was used for all stars as in the previous paper Izmailov & Roshchina (2016). In fact, the value has been the same for all series since 2007. Model parameters x_0, y_0, A, B, C, D, E, where (x_0, y_0) are the coordinates of the center, were calculated with the Non-Linear Least Squares (NLLS). The NLLS algorithm is as follows:

1. Set preliminary model parameters at the zeroth-order approximation.
2. Solve a system of linear equations for the corrections of the parameters.
3. Correct the parameters determined.
4. Repeat from n. 2 until the corrections equal zero with required precision.

Star images obtained with a refractor have a characteristic shape with a sharp peak (Figure 1) due to a residual chromatic aberration; therefore, we used the Moffat function and not the Gaussian or any other more common function. As can be seen from the figure, the Gaussian is not suitable for the approximation of images like this. Using the NLLS, not only can coordinates x_0, y_0 be derived but also their errors. Given that, every night, many CCD-images were taken for each star, those errors were used to calculate weight functions when averaging the relative coordinates during the night. Then, the average annual positions were obtained for each star using the weight functions based on the errors derived in the previous step.

The astrometric reduction, that is, the transition from x_0, y_0 in pixels to the separation in arcseconds and the positional angle in degrees, was made using the six constants method. The six constants are calculated by solving the following system of equations with the method of least

[1] http://izmccd.puldb.ru

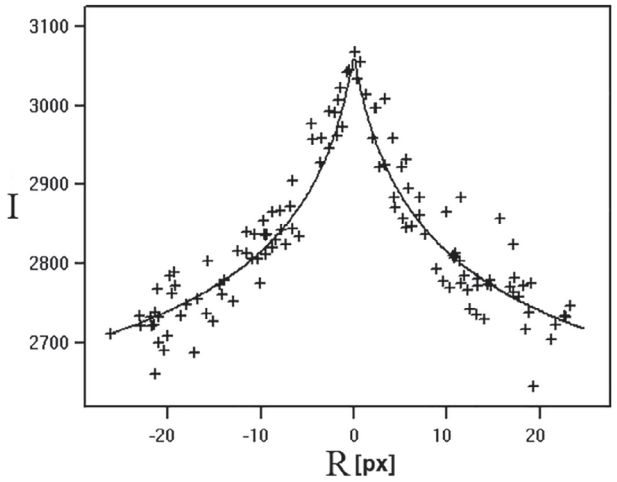

FIGURE 1 Typical star image profile in the focal plane of the 26-inch refractor. Each cross corresponds to a separate pixel. The curve is a model approximation of the image. I—CCD matrix reading. R—the distance from the image center. If a pixel coordinate x is less than the image center coordinate x_0, then $R < 0$; otherwise, $R > 0$

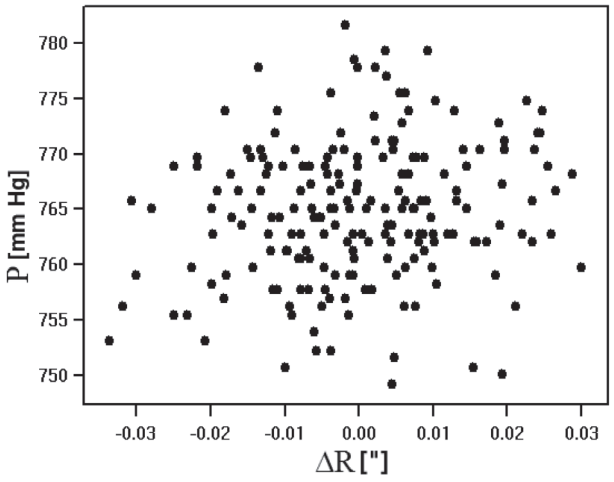

FIGURE 2 The residuals' (ΔR) dependency on the atmospheric pressure in the calibration pair of stars

squares:

$$a_1 x_{0i} + b_1 y_{0i} + c_1 = \xi_i,$$

$$a_2 x_{0i} + b_2 y_{0i} + c_2 = \eta_i,$$

$$i = 1, 2 \ \ldots \ N,$$

where $a_1, b_1, c_1, a_2, b_2, c_2$ are the unknown constants; N is the number of reference stars, each of them corresponding to two equations; x_i, y_i are the coordinates of a reference star with the index i obtained in the previous step; ξ, η are the tangential coordinates of a reference star calculated using the equatorial coordinates from the catalog.

Then, the six constants can be easily converted to scales separately in X and Y directions, coordinate frame shifts in X and Y directions, the tilting angle between two coordinate frames, and the obliqueness of the (X, Y) system (i.e. the angle difference between X and Y axes in relation to 90°). For a detailed description of the method, see Kiselev (1965) and König (1933). To determine those constants, before a main series of images, we used a calibration frame with the 10s exposure. Usually, there are several tens of stars up to 16^m on such frames. Gaia DR2 was used as a reference catalog. As there are bright stars also in the observation program, their images were obtained when the Sun was at least 4.5° under the horizon, that is, during twilight and the period of "white nights" when it is not possible to obtain a CCD-image like that with faint reference stars. In such cases, we use night-averaged values of the scales along x and y and the obliquity of the coordinate system calculated from six constants. We assume it depends linearly on the declination secant (Mikhelson (1976)).

It should be noted that the orbital periods of the observed stars are hundreds and thousands of years. Moreover, observations similar to ours are always distorted by systematic errors, including those depending on the processing techniques. Therefore, we attempt to hold on to as much of the approaches used in our previous works (Izmailov et al. (2010), Izmailov & Roshchina (2016)) as possible.

To analyze the stability of the results obtained, we observed eight pairs of stars with angular distances of 100 arcseconds in addition to the main observation program. We deliberately chose single stars to be able to control the reliability of the above-described methodology of the CCD-frames processing. As shown in the previous paper, even though the scale depends on the air temperature, the usage of the preliminary calibration frame allows us to exclude it from the results. While the temperature–angular distance dependency of one of the reference pairs can be found in that paper, here, we present the distance–atmospheric pressure residuals curve (Figure 2). As can be seen from the figure, there is no correlation between the values. There is also no significant correlation between the coordinate differences and humidity, wind speed, or the line-of-sight distance for all eight pairs. The detailed weather conditions were taken from the data published by the weather station serving the international airport located near the observatory.

Full observation results in a standard format can be downloaded from the Strasbourg astronomical Data Center[2] or the Pulkovo Astrometric online database.[3] Tables 1–3 are fragments of full tables available online.

[2]http://cds.u-strasbg.fr

[3]http://izmccd.puldb.ru/vds.htm

TABLE 1 Relative positions for single observation nights

WDS	Comp.	ADS	T	N	θ (°)	ρ (″)	σ_θ (°)	σ_ρ (″)	$\sigma_{1\tau}$ (″)	$\sigma_{1\rho}$ (″)
…										
02556 + 2652	AB	2218	19.682	2	221.0677	4.6673	0.0715	0.0041	0.0058	0.0041
02556 + 2652	AB	2218	19.684	2	221.4148	4.6718	0.0958	0.0056	0.0078	0.0056
02556 + 2652	AB	2218	19.690	2	221.9291	4.6689	0.1220	0.0069	0.0099	0.0069
02556 + 2652	AB	2218	19.725	2	221.5413	4.6545	0.1030	0.0060	0.0084	0.0060
02581 + 6912		2226	17.708	56	83.0535	3.9695	0.0740	0.0056	0.0380	0.0416
02581 + 6912		2226	19.032	58	82.3619	3.9833	0.0724	0.0059	0.0380	0.0445
03086 + 6028		2359	14.693	5	74.4202	2.1869	0.0952	0.0023	0.0073	0.0046
03086 + 6028		2359	14.701	5	73.8789	2.1729	0.1576	0.0014	0.0120	0.0028
03086 + 6028		2359	14.704	5	73.6318	2.1667	0.0747	0.0016	0.0056	0.0032
03086 + 6028		2359	14.707	5	73.6455	2.1733	0.1090	0.0017	0.0083	0.0034

Note: Tables 1 and 2 contain the following: WDS catalog ID (Mason (2001)); Component IDs from the WDS catalog; ADS catalog ID (Aitken (1932)); T—observation epoch, (2000+); N—number of CCD images; θ—position angle in the coordinate system corresponding to the equator and the equinox of the observation epoch, degrees; ρ—angular distance, arcseconds; σ_θ—position angle error, degrees; σ_ρ—angular distance error, arcseconds; $\sigma_{1\tau}$—error of a single CCD image in the transversal direction $\sigma_\tau[''] = \rho sin\sigma_\theta[^\circ]$, arcseconds; $\sigma_{1\rho}$—error of a single CCD image in the radial direction, arcseconds.

TABLE 2 Average annual positions

WDS	Comp.	ADS	T	N	θ (°)	ρ (″)	σ_θ (°)	σ_ρ (″)	$\sigma_{1\tau}$ (″)	$\sigma_{1\rho}$ (″)
…										
00057 + 4549	AB	48	15.053	1	188.0168	6.0278				
00057 + 4549	AB	48	15.608	3	188.2445	6.0161	0.0081	0.0036	0.0012	0.0051
00057 + 4549	AB	48	16.836	2	188.7521	6.0031				
00057 + 4549	AB	48	17.604	1	189.1507	5.9948				
00057 + 4549	AB	48	19.616	1	189.9584	5.9692				
00059 + 1805	AB	60	14.708	5	134.8426	3.4037	0.0459	0.0032	0.0055	0.0065
00059 + 1805	AB	60	15.647	5	135.0950	3.3893	0.0204	0.0086	0.0024	0.0172
00059 + 1805	AB	60	16.708	5	135.1075	3.4323	0.0203	0.0073	0.0024	0.0146
00059 + 1805	AB	60	17.797	6	135.3700	3.4242	0.0359	0.0069	0.0048	0.0153

Note: Table 2 labels are equivalent to those of Table 1 with the exception of: N—number of observation nights; $\sigma_{1\tau}$—error of a single CCD image in the transversal direction $\sigma_\tau[''] = \rho sin\sigma_\theta[^\circ]$, arcseconds; $\sigma_{1\rho}$—error of a single observation night in the radial direction, arcseconds.

Table 1 shows the relative positions of the binaries' components for single nights. Table 2 contains average annual positions. For stars with already defined orbits, the differences between observed and precalculated positions (O-C) can be found in Table 3. Please note that the position angle is presented in the coordinate system corresponding to the equinox of the observation epoch, and not J2000. The position angle errors ($\sigma_{1\tau}$) are presented in arcseconds, which allows for a direct comparison with the angular distance errors ($\sigma_{1\tau}$ is calculated as an angular distance in the transversal direction in arcseconds, corresponding to $\sigma_{1\theta}$ in degrees).

Figures 3 and 4 represent the observed minus ephemeris values from Table 3 in separation $(O-C)_\rho$ and position angle $(O-C)_\theta$ in arcseconds as a function of separation ρ obtained using the calculated orbits from different sources. We chose logarithmic scales as the separation between components, as well as the quality of the star images, varies significantly. We used the following formula: $y = \pm\ln(|O-C|+1)$, where y is the y-axis value, and the sign plus or minus represents the sign of the corresponding (O–C) value. Hence, if (O-C) equals zero, then $y = 0$ as well. As the figures show, there is no bias or any correlation between our orbits and the other

TABLE 3 The differences between observed and precalculated positions (O–C)

WDS	Comp.	$(O-C)_\rho$ ($''$)	$(O-C)_\theta$ (°)	$(O-C)_{\Delta\theta}$ ($''$)	Abbrev.
00184 + 4401	AB	0.0594	−0.4901	−0.2934	PkO2014c
00360 + 2959	AB	−0.0323	0.4750	0.0521	Kis2009
03162 + 5810	AB	0.0413	0.3680	0.0323	Zir2008
08369 + 2315		−0.0130	0.2871	0.0133	Hrt2011d
09013 + 1516	AB	−0.0035	0.2485	0.0218	Zir2008
09414 + 3857	AB	−0.0200	0.2777	0.0135	Lin2013a
09524 + 2659		−0.0378	−0.1690	−0.0073	Lin2016a
11,387 + 4507	AB	0.0768	0.2525	0.0394	Hle1994
12,244 + 2535	AB	−0.0314	1.6551	0.0523	Ole2000b
12,272 + 2701	AB	0.0167	0.3976	0.0191	Ole2003b

Note: Table 3 columns contain the following: WDS catalog identifier; Component IDs from the WDS catalog; $(O-C)$ by angular distance ρ, arcseconds; $(O-C)$ by position angle θ, degrees; $(O-C)$ by position angle θ ($\Delta_\tau[''] = \rho sin\Delta_\theta[°]$), arcseconds; Abbreviated reference to the original publication in the WDS where the orbit elements are given.

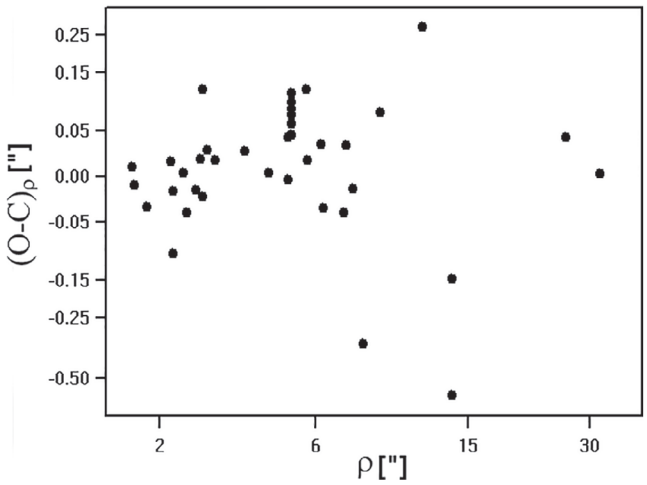

FIGURE 3 $(O-C)_\rho$ as a function of separation on a logarithmic scale (see the text) in arcseconds. The ephemeris values are calculated using orbits from the literature

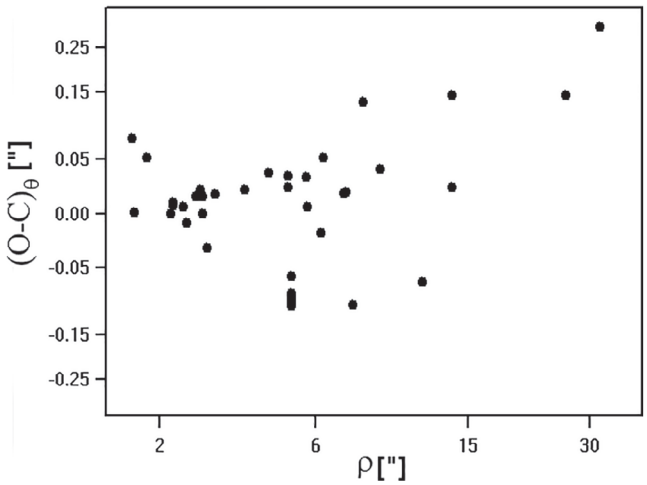

FIGURE 4 $(O-C)_\theta$ as a function of separation on a logarithmic scale (see the text) in arcseconds. The ephemeris values are calculated using orbits from the literature

data. Similarly, there is no correlation between the $(O-C)$ values and the position angles, as well as the equatorial coordinates of stars. It is natural that there are no dependencies between the $(O-C)$ values and both the observational errors and the accuracy of the calculated orbits. It should be noted that the $(O-C)$ values usually significantly exceed the observational errors presented in Tables 1 and 2. It can be explained by either the lack of orbits that need improvement or the existence of systematic errors in observations. Below, we made an attempt to reveal the systematic errors by making a comparison between our data and the Gaia DR2 data.

3 | COMPARISON WITH OTHER OBSERVATIONS AND DISCUSSION

As mentioned previously, the main goal of the binaries observation program with the 26-inch refractor is to achieve the highest possible precision of relative positions series. For some stars of our observation program, there are positions series obtained with the 26-inch Washington refractor (W26) (Mason et al. (2018)) and 102-cm Zeiss telescope of the Brera Astronomical Observatory equipped with the Pupil Interferometry Speckle camera and COronagraph (PISCO) (Scardia et al. 2018).

TABLE 4 Comparing the accuracy of observations made with the 26-inch Pulkovo refractor, the 26-inch Washington refractor, PISCO, and SOAR

	Std Dev (θ) (*mas*)	Std Dev (ρ) (*mas*)	N
PISCO	8.13	19.49	8
PUL26	7.16	8.71	8
W26	27.57	48.79	30
PUL26	7.63	9.75	30
SOAR	10.77	7.37	18
PUL26	7.21	8.48	52

The accuracy of the final results depends in a complex way on the separation between binary components, the magnitude of the brightest star, the magnitude difference between components, etc. Therefore, the best way to compare accuracy is to analyze observation series of the same objects. Table 4 shows the comparison of the average accuracy of eight simultaneous observation series obtained with PISCO and 30 Washington refractor series. The accuracy was defined as a standard deviation from the linear approximation of the relative motions in a pair of stars separated in distance and position angle. For the Washington refractor, the observations from 2000 to 2017 were used, for PISCO from 2004 to 2015, and for Pulkovo refractor from 2003 to 2019. It should be noted that this is the accuracy of long-term observations, and another estimation method can yield different results. Thus, in a recent paper on observational results from the Washington refractor (Mason et al. 2018, one of the estimation criteria is $d\rho/\rho = 0.0020$. As shown in Table 4, the Pulkovo series have some advantage over the Washington series. It becomes even more evident when analyzing the observations of single stars. Figure 5 presents relative positions of a well-known binary mu Dra obtained with three instruments in the 21st century. Figure 6 presents the same positions from all world observations. Unfortunately, there are no mutual long-term observations of the same objects made with the Pulkovo refractor and the $4.1 - m$ Southern Astronomical Research (SOAR) telescope located on Cerro Pachón, Chile (Tokovinin et al. (2019)). However, there is an intersection over the range of separations between components. Binaries with separations from $1''.5$ to $2''.9$ were observed with both instruments. There are long-term series for 18 stars observed with the SOAR telescope and for 52 stars observed with the Pulkovo refractor. As can be seen in Table 4, the accuracy is similar.

In the field of astrometry under consideration, the question that has been debated frequently is whether the observing instrument or the methodology of CCD image processing contributes more to the high accuracy

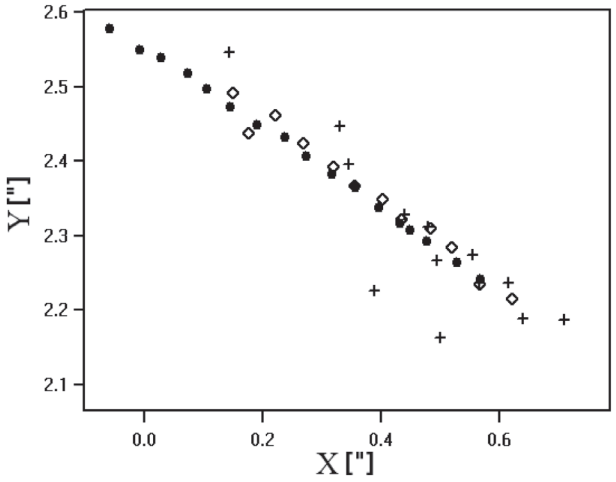

FIGURE 5 The relative positions of μDra B (μDra B is located at 0.0) from the observations with the 26-inch refractor (circles), 26-inch Washington refractor (crosses), and PISCO (rhombs), starting from 2000

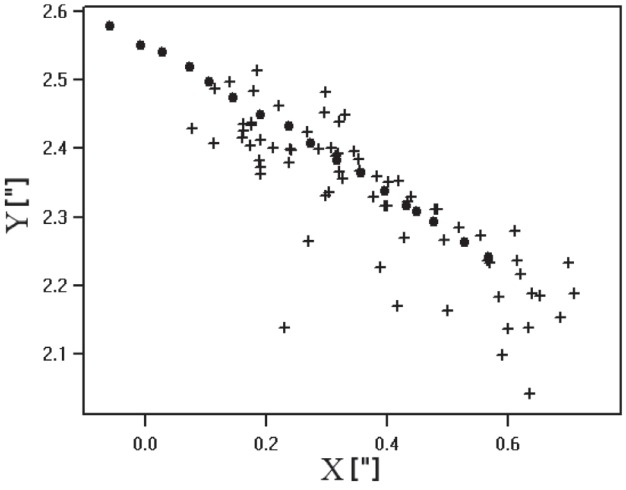

FIGURE 6 In the picture plane (X, Y): all observations of μ Dra in the literature at present, starting from 2000, with the 26-inch Pulkovo refractor (circles) and all other telescopes (crosses)

of the relative positions. For an independent analysis, two binaries, 61Cyg (ADS14636) and ADS683, were observed simultaneously using the Meniscus Maksutov Telescope (MTM-500, $D = 500$ mm, $f = 6{,}500$ mm) of the Crimean Astrophysical Observatory. The telescope is equipped with the Apogee FW50-9R CCD camera, which allows for a $12' \times 12'$ field of view and $0''.725$ pixel size. The results are presented in Table 5. The nomenclature is equivalent to the one used in Table 2. Worth noting is the position angle difference of $0°.153$ for 61 Cyg, which corresponds to the $0''.084$ for this separation between components. We assume that the difference has the nature of a systematic error associated with the telescope. As shown in Table 5, the accuracy is similar. Compared telescopes have

TABLE 5 Comparison of the results of the simultaneous observations with the 26-inch Pulkovo refractor and MTM-500

	Object	T	θ (°)	ρ ($''$)	σ_τ ($''$)	σ_ρ ($''$)	N
MTM-500	ADS683	19.763	295.3793	4.2568	0.0058	0.0197	10
PUL26	ADS683	19.763	295.4492	4.2727	0.0078	0.0106	5
MTM-500	61Cyg	19.782	153.0328	31.8349	0.0064	0.0083	10
PUL26	61Cyg	19.782	153.1843	31.8353	0.0084	0.0162	26

TABLE 6 Comparison of the results to Gaia DR2

	x (*mas*)	y (*mas*)	μ_x (*mas/yr*)	μ_y (*mas/yr*)
Δ	2.076	−3.544	0.447	0.369
σ_o	23.122	23.800	7.218	10.243
σ_c	2.788	2.964	0.698	0.725

Note: Δ—average differences; σ_o—standard deviation of a single difference; σ_c—the average error of a single difference calculated using the errors of subtracted values; x, y—parameters in the direction of the right ascension and the declination; μ_x, μ_y—proper motion parameters in the direction of the right ascension and the declination.

TABLE 7 Comparison to the ephemerides calculated using orbits from Izmailov (2019)

	τ (*mas*)	ρ (*mas*)
Δ	−1.909	7.783
σ_o	10.510	20.534
σ_c	5.200	8.600
Δ_a	4.969	−0.426
σ_{ao}	90.818	131.019

Note: τ, ρ—parameters in the direction of the position angle change and the separation (e.g. $\Delta_\tau = \rho sin\Delta_\theta$); Δ_a and σ_{a0} are associated with orbits from the 6th orbit catalog (Hartkopf and Mason, 2001); Other labels are equivalent to those of Table 6.

significantly different constructions, including different optical circuits, but the observational results, at least in accuracy, are almost identical. With that in mind, we can conclude that, in the case of comparable apertures and cameras, observation processing has a decisive impact on the quality of the results.

Gaia DR2 catalog contains data for all binaries under investigation. This allows us to compare obtained data both by positions and proper motions (see Table 6).

All parameters are calculated for 290 mutual binaries. As well as in Scardia et al. (2018), the coordinate differences in our data are ∼100 mas for some stars. The difference between standard deviations and average errors of the parameters indicates that unknown systematic errors take place. We have not found any dependencies of the position differences and proper motions on star magnitudes; magnitude differences in a pair in G, BP, or RP bands; effective temperature of the main component; or effective temperature differences in a pair.

In Izmailov (2019), the ephemerides for distances and position angles of the 2019.0 epoch and their errors were published for some of the binaries. The obtained data allow us to make a comparison; see Table 7.

The observational results of the 2019.0 epoch were evaluated with the linear time approximation of several average annual values ρ and θ. As can be seen from Table 7, as well as when compared to Gaia DR2 data, precalculated errors are better than real differences. It confirms the existence of systematic errors caused by unknown factors.

To clarify, when comparing σ_o and σ_c, we presume the following. Let us say there are two observation series of the same binary. If we calculate ρ differences, we can directly derive mean difference estimate and standard deviation (σ). On the other hand, the standard deviation estimates of ρ are known (σ_1 and σ_2). If cross-covariances of the series are insignificant, and there are no systematic errors caused by unknown factors, we can expect $\sigma^2 \approx \sigma_1^2 + \sigma_2^2$. The comparisons made by us show that this condition is ruled out ($\sigma^2 > \sigma_1^2 + \sigma_2^2$), which suggests that there are unknown systematic shifts between the observation series. For more information on statistic methods, see Wielen (1997).

We should note that the average accuracy of a single observation can be derived as the mean value of $\sigma_{1\rho}$ and $\sigma_{1\tau}$ throughout Table 2, which equals $0''.013$ and $0''.0077$, respectively. Here, $\sigma_{1\tau}$ is simply an arc length in the tangential direction of a position angle in arcseconds, and it can be easily converted to degrees: $\sigma_{1\theta}[^\circ] = \sigma_{1\tau}[''] * 180[^\circ]/(\pi\rho[''])$. Using this equation, we can derive $\sigma_{1\theta} = 0^\circ.44/\rho$ where ρ is the angular distance in arcseconds.

4 | CONCLUSIONS

As indicated above, the obtained results are sufficiently accurate and can be used for orbit determination

techniques, including the method of apparent motion parameters. However, we believe that the problem of systematic errors requires further investigation. In particular, an explanation is needed for the presence of significant occasional deviations at the level of 100 mas between the Gaia data and our results, taking into account the fact that the accuracy of our observations is much better than 100 mas. As such deviations are also present in other studies, they cannot be attributed to rough errors made during observations or processing. For now, the observations of visual binaries with the 26-inch Pulkovo refractor continue.

ACKNOWLEDGMENTS

This work features data from the Washington Double Star Catalog (WDS) of the United States Naval Observatory. The authors express deep gratitude to the WDS creators. This work has made use of data from the European Space Agency (ESA) mission *Gaia*,[4] processed by the *Gaia* Data Processing and Analysis Consortium[5] (DPAC). Funding for the DPAC has been provided by national institutions, particularly the institutions participating in the *Gaia* Multilateral Agreement. The study was undertaken with the financial support of the Russian Foundation for Basic Research under Contract No. 20-02-00563A.

REFERENCES

Aitken, R. G. 1932, *Visual Double Stars: Formation, Dynamics and Evolutionary Tracks*, Carnegie Institute (Washington, DC).

Brown, A. G. A., Vallenari, A., Prusti, T., de Bruijne, J. H. J., Babusiaux, C., & Bailer-Jones, C. A. L. 2018, *A&A*, *616*, 1.

Izmailov, I. S. 2019, *Astron. Lett.*, *45*, 30.

Izmailov, I. S., & Roshchina, E. A. 2016, *Astrophys. Bull.*, *71*(2), 225.

Izmailov, I. S., Vinogradov, V. S., & Rumyantsev, K. V. e. a. 2004, *Pulkove*, *217*, 536.

Izmailov, I. S., Khovricheva, M. L., & Khovrichev, M. Y. e. a. 2010, *Astron. Lett.*, *36*(5), 349.

Kiselev, A. A. 1965, *Astron. Rep.*, *9*(2), 354.

Kiselev, A. A., & Romanenko, L. G. 2011, *Astron. Rep.*, *55*(6), 487.

Kiselev, A. A., Romanenko, L. G., & Gorynya, N. A. 2009, *Astron. Rep.*, *53*(2), 1136.

Kiselev, A. A., Kiyaeva, O. V., Romanenko, L. G., & Gorynya, N. A. 2012, *Astron. Rep.*, *56*(7), 524.

Kisselev, A. A., Romanenko, L. G., & Kalinichenko, O. A. 2009, *Astron. Rep.*, *53*(12), 126.

König, A. 1933, in: *Handbuch der Astrophysik*, ed. W. E. E. A. Bernheimer, Springer (Berlin, Heidelberg), 502.

Mason, B. D. 2001, *The Washington Double Star Catalog*, United States Naval Observatory (Washington, DC).

Mason, B. D., Hartkopf, W. I., Urban, S. E., & Josties, J. D. 2018, *Aston. J.*, *156*(5), 240.

Mikhelson, N. N. 1976, *Optical Telescopes: Theory and Design*, Izdatel'stvo Nauka (Moscow).

Moffat, A. F. J. 1969, *A&A*, *3*, 455.

Romanenko, L. G., & Kiselev, A. A. 2014, *Astron. Rep.*, *58*(1), 30.

Scardia, M., Prieur, J.-L., Pansecchi, L., Argyle, R. W., Zanutta, A., & Aristidi, E. 2018, *Astron. Nacher.*, *339*, 571.

Shakht, N. A., Gorshanov, D. L., Grosheva, E. A., Kiselev, A. A., & Polyakov, E. V. 2010, *Astrophysics*, *53*(2), 227.

Tokovinin, A., Mason, B. D., Mendez, R. A., Horch, E. P., & Briceño, C. 2019, *Astron. J.*, *158*(1), 48.

Trifonov, T., Tal-Or, L., Zechmeister, M., Kaminski, A., Zucker, S., & Mazeh, T. 2020, *A&A*, *636*, 74.

Wielen, R. 1997, *A&A*, *325*, 367.

How to cite this article: Izmailov I, Rublevsky A, Apetyan A. Astrometric observations of visual binaries using 26-inch refractor at Pulkovo Observatory during 2014–2019. *Astron. Nachr.*. 2020;1–8. https://doi.org/10.1002/asna.202013815

[4]https://www.cosmos.esa.int/gaia

[5]https://www.cosmos.esa.int/web/gaia/dpac/consortium